12-2014

Conceptual Groundwater Model of Sea Level Rise in the Humboldt Bay Eureka-Arcata Coastal Plain

Robert Willis

Conceptual Groundwater Model of Sea Level Rise in the Humboldt Bay Eureka-Arcata Coastal Plain

Prepared for

State Coastal Conservancy
1330 Broadway, 13th Floor
Oakland, CA 94612-2530

Coastal Ecosystems Institute of Northern California
PO Box 806
Bayside, CA 95524

Prepared by

Robert Willis, Ph.D.
Arcata, CA 95521

Final Report

December 2014

Table of Contents

1 Introduction

The objective of this study is to develop a conceptual groundwater model to analyze projected sea level rise (SLR) in the Eureka–Arcata coastal plain (the study area). The goal is to provide the Humboldt Bay Sea Level Rise Adaptation Planning (HBSLRAP) project preliminary information concerning possible SLR effects on groundwater.

The U.S. Geological Survey's (USGS) mathematical model, SUTRA (Saturated-Unsaturated-Transport), is used to analyze the possible impacts associated with SLR (1). The mathematical model simulates flow and transport (water quality) in a representative, two dimensional, cross-section, in the Eureka–Arcata plain.

The mathematical model is a conceptual model of the locally, shallow unconfined aquifer. The conceptual model is not a calibrated or validated model; the hydrologic and geohydrologic data requirements of such an investigation far exceed the time and budgetary limitations of the present study. The conceptual model is used to simulate the possible impacts of SLR in the study area. The magnitude, timing, reliability and accuracy of these impacts can only be assessed with additional geohydrologic data and more general mathematical models.

The following sections of this report discuss the literature on SLR and groundwater simulation, the mathematical model, and the results and conclusions of the study.

2 Literature Review

2.1 Simulation Models

The principal models used for the simulation of coastal saltwater intrusion and SLR have been MODFLOW (2), SUTRA, and SEAWAT (3). MODFLOW is a quasi-three dimensional circulation model based on finite difference approximations of the underlying groundwater flow equations. MODFLOW, in contrast to SUTRA, analyzes groundwater flow in a series of layers; within each layer the flow is horizontal. SEAWAT may be used with MODFLOW to simulate, approximately, saltwater intrusion.

Tony and Sindu (4) analyzed potential SLR in the coastal region of Thiruvananthapuram, India. SLR's impact on groundwater levels was determined to have a minor impact on groundwater levels. MODFLOW and SEAWAT were used by Chang (5) to analyze SLR in coastal aquifers. The conceptual simulation results indicated no long-term impact on aquifer systems. Sensitivity analyses indicated that variation in the rainfall can impact the saltwater intrusion process.

Saltwater intrusion in the Ewa area of Oahu, Hawaii was simulated using SUTRA (6). A cross-sectional, density-dependent, flow and transport model analyzed the flow in the layered sedimentary aquifer. Similar applications have been presented in (7) and (8).

Loaiciga et al. (9) applied a three-dimensional, finite element model to the Seaside area sub-basin near Monterey, California to assess SLR. Various scenarios regarding groundwater pumping and SLR were analyzed with the simulation model. The results indicated an "expanded zone of sea water intrusion." (9, pg. 46). It should be noted that groundwater extractions under post-2006 baseline conditions total 15,340 m^3/day.

Masterson and Garabedian (10) analyzed SLR using SEAWAT, a density dependent, three dimensional groundwater flow model for a hypothetical fresh-water lens. The aquifer was a conceptual model, representative of shallow, coastal aquifers along the United States' Atlantic coast. The simulation results showed that the decline in groundwater levels relative to SLR is directly related to the "proximity of groundwater fed streams and whether the streams are tidally influenced" (10, page 217).

Webb and Howard (11) used SEAWAT in the analysis of SLR. The results of the two-dimensional study, indicated that aquifers with a low ratio of hydraulic conductivity to recharge, and low porosity, stabilized within decades following the cessation of SLR; in the other extreme, systems could take several centuries to achieve a new equilibrium. Rasmussen et al. (12) analyze the vulnerability of groundwater abstraction resulting from climate change and SLR. MODFLOW and SEAWAT were using to simulate sea water intrusion for an island in the western Baltic Sea. The results of the study show that intrusion is sensitive to changes in sea level and groundwater recharge and the stage of drainage canals. Boundary conditions also may have a major role in the impacts.

Werner and Simmons (13) present a simple conceptual model to analyze SLR in coastal aquifers. The analysis presumes steady-state conditions. The study demonstrated that the upper bound for "sea water intrusion due to sea-level rise is no greater than 50 m" migration of the saltwater toe (13, page 197).

A two-dimensional numerical model was used to simulate saltwater intrusion for a range of SLR scenarios in Broward County, Florida (14). The SEAWAT results indicated that the severity of intrusion is "largely" related to SLR over the next 100 years. Nishikawa et al. (15) applied SUTRA to the Dominquez Gap area in Los Angeles. The simulation results indicated than an instantaneous 1 m SLR may accelerate seawater intrusion assuming there is no change in current water management strategies. MODFLOW was used to assess SLR in New Haven, Connecticut (16). The results from the steady-state simulation model indicated that groundwater levels can be expected to increase in the coastal area especially if groundwater recharge increases.

Numerical simulation models have also been used to study SLR in the Mediterranean and Dead Sea coastal aquifers (17). The impact of SLR in this region is a function of the coastal topography. Increased overdraft of groundwater and/or reduced recharge will also increase saltwater intrusion. MODFLOW and SEAWAT were used in a New York study to address SLR (18). The models incorporated rainfall and SLR changes. Both the water table and the degree of

saltwater intrusion increased. Similar results are presented in (19) using SUTRA. In this study, sea water intrusion can be expected to increase if groundwater overdraft continues.

2.2 Groundwater Data

The application of any groundwater model is dependent on the quality and the quantity of data. In the development of a SLR model of the Eureka–Arcata plain a number of data sources were consulted. The baseline geology and groundwater assessment was initially surveyed by Evenson in 1959 (20). The report delineates the principal geologic units in the area and the groundwater resources. The U.S. Geologic Survey and the California Department of Water Resources (DWR) have also published a number of reports detailing the groundwater resources of the State including quantity and quality of groundwater, and an inventory of groundwater data (21, 22, 23). DWR's California Water Plan for the North Coast contains general hydrologic data as well as flood management and regional water conditions (supplies, quality, and governance) (24, 25).

A series of maps were also identified that provided baseline information on the local geology (26, 27, 28). Generalized cross-sections and a summary of geologic formations are presented in (29, 30). Well data are available from the California Department of Water Resources in the Eureka-Arcata Plain (31). Typically water levels are measured bi-annually. These data are useful in identifying trends; the data are of little value in calibrating a transient simulation model. Furthermore, the temporal and spatial variation in groundwater withdrawals are unknown.

Precipitation, evapotranspiration, and streamflow are available from the National Climatic Data Center (NCDC) (32), the California Irrigation Management Information System (CIMIS) (33), and the California Data Exchange Center (CDEC) (34).

3 Simulation Model

The USGS simulation model used in the study is SUTRA (1). The model was selected to simulate the coastal aquifer hydraulics and mass transport in a vertical cross-section of the study area. Assuming an isothermal and fully saturated aquifer, the governing equations are (1) total fluid density equation:

$$\rho = \rho_0 + \frac{\partial \rho}{\partial C}(C - C_0) \tag{1}$$

where ρ is the fluid density, ρ_0 is the base fluid density at concentration C_0; C_0 is the mass fraction of mass solute per unit mass of the total fluid.

(2) Darcy's law:

$$\mathbf{v} = -(\frac{\mathbf{k}}{n\mu}) \cdot (\nabla p - \rho \mathbf{g}) \tag{2a}$$

where $\mathbf{v}$ is the average fluid velocity, $\mathbf{k}$ is the intrinsic permeability matrix, p is the fluid pressure, n is the porosity, μ is the viscosity, and $\mathbf{g}$ is the gravity vector.

(3) The mass conservation equation (assuming no additional sources or sinks of mass):

$$\frac{\partial(\rho n)}{\partial t} = -\nabla \cdot (n\rho \mathbf{v}) \tag{2b}$$

(4) Solute mass balance:

$$\frac{\partial(n\rho C)}{\partial t} = -\nabla \cdot (n\rho \mathbf{v} C) + \nabla \cdot [n\rho (D_m I + \mathbf{D}) \cdot \nabla C] + S^* \tag{3}$$

where D_m is the molecular diffusivity of the solute, I is the identity tensor, S^* is a source/sink term, and $\mathbf{D}$ is the dispersion tensor.

Further details of the underlying assumptions and parameter representations $(\mathbf{D}, \mathbf{k})$ may be found in (1) and (36).

3.1 Boundary and Initial Conditions

The boundary conditions of the cross-sectional model requires information on the pressure field, p, and the mass fraction, C, on the perimeter of the system. Dirichlet boundary conditions specify values of both p and C; the boundary conditions can be time-varying. Neumann boundary conditions are flux boundary conditions. In SUTRA they can be approximated using a series of point sources (1, pg. 169).

The initial conditions prescribe for a transient simulation, the pressure and concentration field throughout the spatial domain at the inception of the simulation.

3.2 Numerical Model

The governing equation of flow and transport are nonlinear partial differential equations. These equations are approximated in SUTRA using finite elements. The temporal derivatives are represented using finite differences. Further details of the numerical solution of the model may be found in the SUTRA documentation (1, Chapter 4).

4 Model Application

The SUTRA cross-sectional model was applied to the study area. The study area shown in Figure 1 extends from approximately Guintoli Lane to the coast, the location where the mean sea level elevation is zero. Also shown are the locations of 3 DWR wells; data for the wells are summarized in Table 1. The horizontal datum for all wells is NAD83; the projection is UTM and the units are meters. Note that none of the wells coincide with the assumed cross-section, and that the daily extraction rates are unknown.

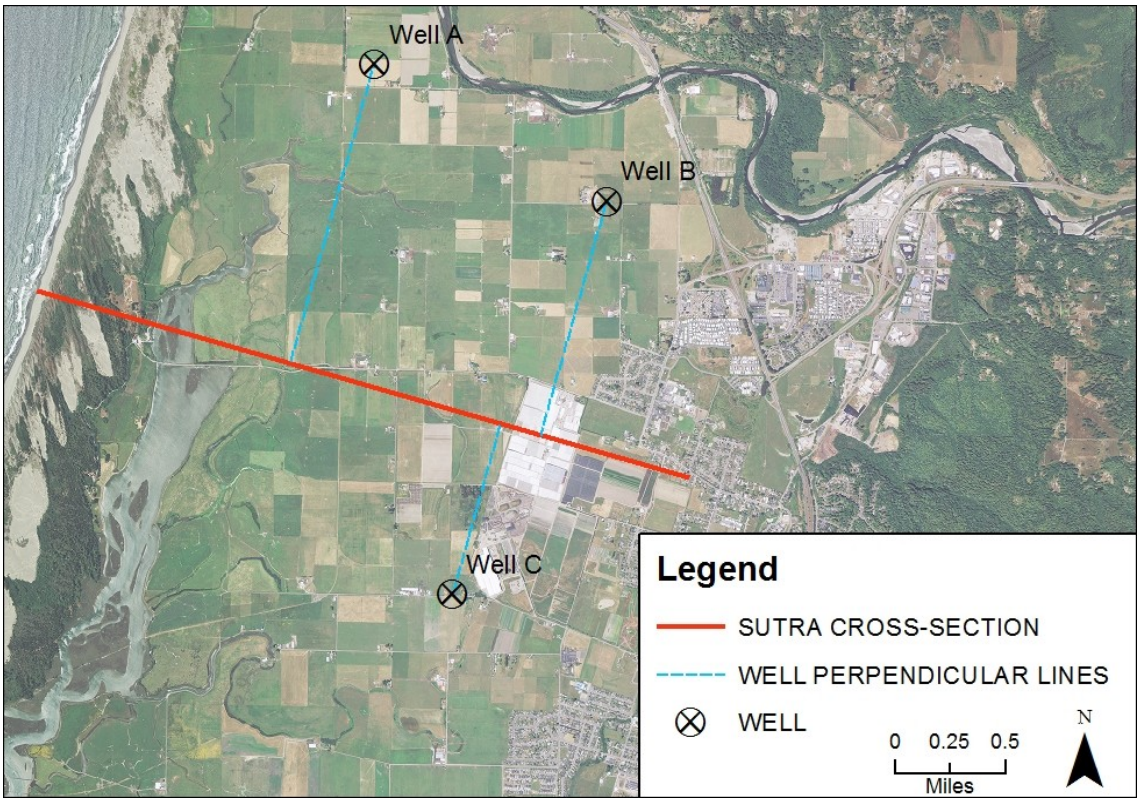

Figure 1 **Humboldt Bay Eureka-Arcata coastal plain study area showing location and extent of SUTRA cross-section, and location of 3 Department of Water Resource wells.**

Table 1 **DWR Well Data**

Model Well Identifier	State Well Number	Easting	Northing
Well A	06N01E07M001H	405876	4530197
Well B	06N01E17D001H	407571	4529211
Well C	06N01E19Q001H	406443	4526378

The assumed length of the cross-section is 5000 m (Figure 1); the thickness of the aquifer is 30 m. The cross-section's dimensions were developed in collaboration with Northern Hydrology & Engineering (34). The finite element grid (network) is shown in Figure 2. The origin of the coordinate system of the grid is the lower left corner of the Figure ($x = 0, z = 0$ meters), corresponding to the eastern boundary of the study area.

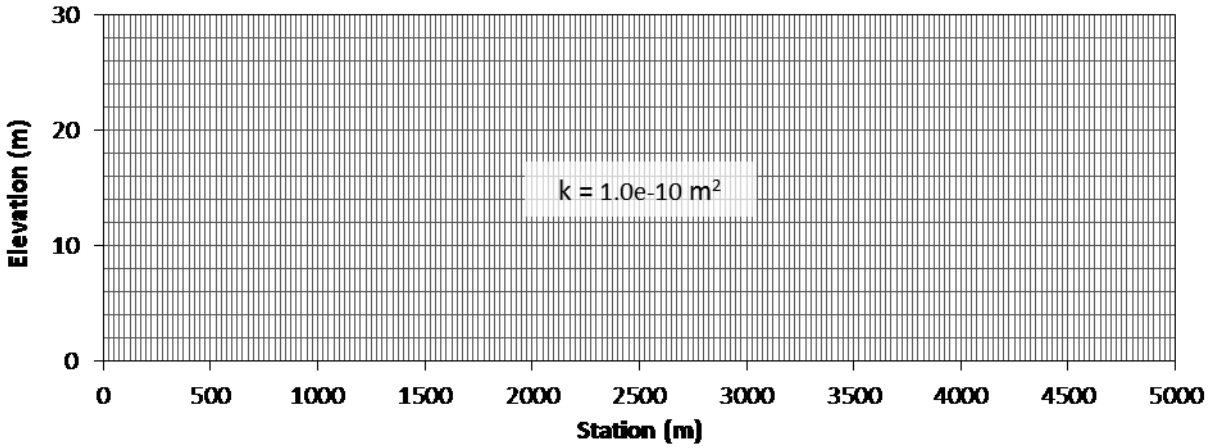

Figure 2 Finite element network for Scenario 1 and 2 with homogenous aquifer.

Additional aquifer and numerical parameter data are presented in Table 2. The dispersivity parameters are components of the dispersion coefficient. The estimated recharge is developed from NCDC and CIMIS data sources. In SUTRA, the recharge rates were simulated using a series of recharge wells located on the top boundary of the aquifer ($z = 30$ m).

An important element of the simulation are the boundary conditions. On the ocean side of the study area, hydrostatic pressure was assumed. The pressure was calculated as

$$p = \rho g z \tag{4}$$

where ρ is the density of saltwater 1024.99 kg/m^3 , and z is the elevation above the base of the aquifer. The specified concentration on the seawater boundary is assumed to be saltwater, $C_{sea} = 0.0357$ [kg (dissolved solids/kg (seawater)]. On the east side of the study area, the boundary conditions was also hydrostatic. However, it was necessary to add a head or pressure differential to the boundary pressure. This differential was determined through repeated simulation to best replicate the average water levels in Wells A, B, and C. This Δh is shown in Table 2.

Table 2 Parameters

Parameter	Units	Value
Intrinsic Permeability ($\mathbf{k}$)	m^2	1.e-10
Intrinsic Permeability Bay Sediments ($\mathbf{k}$)	m^2	1.e-12
Molecular Diffusivity ($\mathbf{D}$)	m^2/s	18.8571e-6
Longitudinal Dispersivity	m	10
Transverse Dispersivity	m	1
Porosity		0.3
Recharge Rate	kg/s	0.0205
Head Delta East Boundary (Δh)	m	3.6
Number of Finite Elements		3216
Time Step	days	0.1

5 Model Results

The simulation model was used to analyze the SLR scenarios at steady-state assuming the aquifer is homogeneous and isotropic; there is no spatial variation in the intrinsic permeability. The transient simulation model continues until the mass balances indicated a net change of zero in mass storage, e.g. steady-state. This occurred within 25-30 years of simulation time. This also eliminates the initial conditions from playing any role in the transient simulation results. The SLR saltwater boundary condition was applied instantaneously at the beginning of the simulation.

The results will examine five scenarios. The first scenario examines the steady-state pressure and concentration distribution resulting from SLR of 0, 1, and 2 meters in a homogeneous aquifer (Figure 2). In the second case, the aquifer is no longer homogeneous. A series of Bay deposits are incorporated in the cross-sectional model. The deposits have an intrinsic permeability two order of magnitude smaller than the alluvial materials (Table 2). The Bay materials extend from $x = 2500$ to $x = 4500$ meters (34). The thickness of the deposits ranges from 15 meters in the second scenario to 22.5 m in the third scenario (Figure 3). The fourth scenario simulated a 125 year transient simulation. In this fourth scenario, SLR is simulated as a time dependent boundary condition that varies linearly over a 100 year period; a maximum 2 m SLR is assumed. The aquifer is homogeneous; there are no Bay materials. The fifth scenario examines a potential worst-case scenario. In this simulation, the natural recharge is 50% of the long-term average, and the Bay materials are 75% of the aquifer's thickness. SLR is 2 m.

The simulation results, presented in Table 3and Table 4, are discussed below.

Table 3 Saltwater Intrusion Impacts

Scenario	SLR (m)	50% Isochlor	SLR (m)	50% Isochlor	SLR (m)	50% Isochlor
1	0	4871	1	4767	2	4696
2	0	4752	1	4702	2	4642
3	0	4669	1	4612	2	4551
5					2	4396

Table 4 Maximum Head Impacts

Scenario	SLR (m)	Max h (m)	X (m)
1	0	3.59	0
1	1	3.59	0
1	2	3.63	825
2	0	3.59	0
2	1	3.61	650
2	2	3.77	1650
3	0	3.70	1275
3	1	3.83	1850
3	2	4.01	2525
5	2	3.70	1800

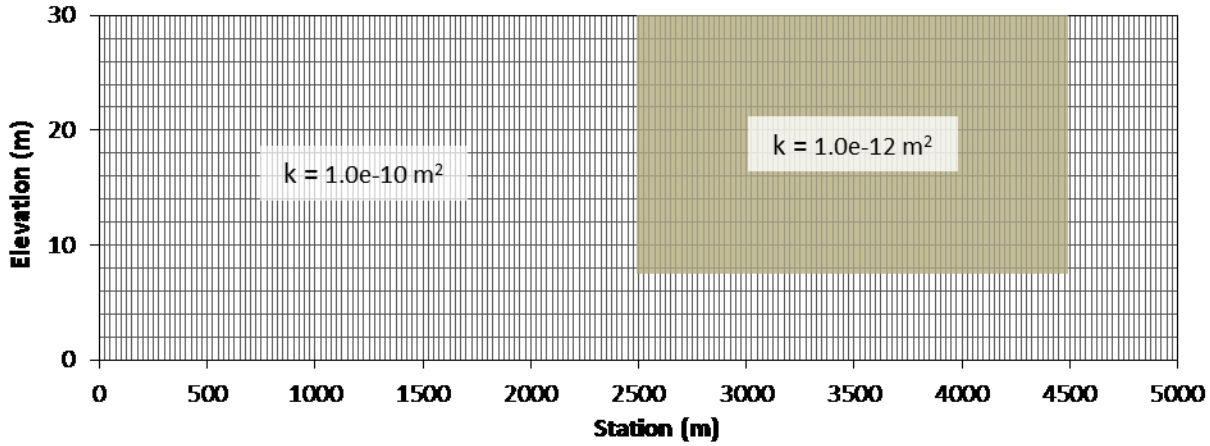

Figure 3 **Finite element network for Scenario 3 and 5 with non-homogenous aquifer.**

5.1 Scenario 1 Results

Figure 4 depicts the hydraulic head (water level, $z = 30$ m) versus the distance from the eastern boundary; the coastal boundary is located at $x = 5000$ m. The consequence of SLR is that the hydraulic head increases throughout the system. A 2 m increase in SLR at the coastal boundary shifts the maximum head westward to approximately $x = 825$ m; the maximum head is 3.6 m. As shown in Figure 4, the 2 m SLR increases the overall water level in the aquifer. The water levels exceed the eastern boundary condition head over a horizontal distance of approximately 1500 m. This does not occur under the baseline condition and the 1 m SLR scenario.

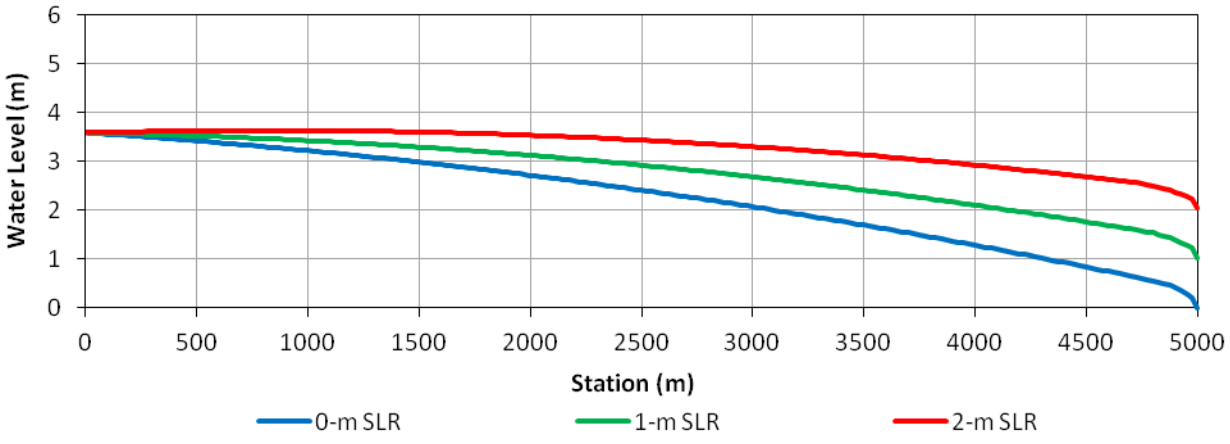

Figure 4 **Scenario 1 water levels for 0, 1, and 2 m of sea level rise.**

Saltwater intrusion is also increased with SLR. The baseline conditions of the aquifer show minor saltwater intrusion. Intrusion is controlled by the magnitude of freshwater outflow of the aquifer. This outflow is a function of the hydraulic gradient, the difference in the hydraulic head

between the eastern and coastal boundaries. Recall that the eastern boundary condition was determined by adjusting the Δh over and above hydrostatic conditions to approximate the mean annual water levels in Wells A, B, and C.

A measure of saltwater intrusion is the location of the 50% isochlor as it intersects the base of the aquifer, $z = 0$ m. For baseline conditions, this occurs at approximately $x = 4871$ m. A 1 m increase in SLR, shifts the 50% isochlor eastward to $x = 4767$ m. The location of the 50% isochlor for a 2 m SLR is $x = 4696$ m. Seawater intrusion, as represented by the 50% isochlor, has increased by over 175 m in the 2 m SLR scenario. Figure 5 illustrates a typical seawater intrusion profile; note that the vertical scale is exaggerated by a factor of 100.

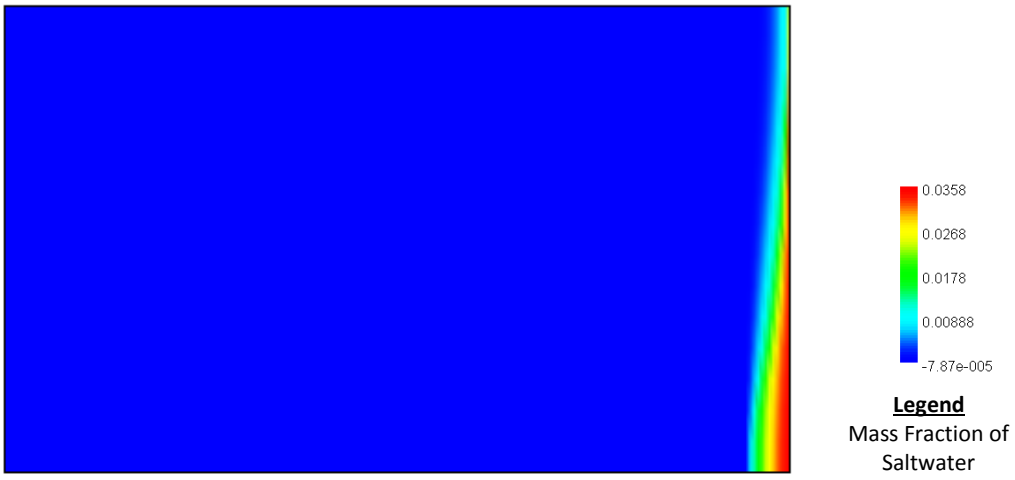

Figure 5 **Scenario 3 saltwater intrusion for 2 m of sea level rise over model domain. Seawater is red and blue is freshwater.**

5.2 Scenario 2 Results

Scenario 2 analyzes the impacts of homogeneity in the intrinsic permeability. In this Scenario, Bay materials (muds) are assumed to occur from $x = 2500$ m to $x = 4500$ m (35). The thickness of the deposits, which have significantly smaller intrinsic permeability, is 50% of the total aquifer thickness (30 m).

The impact of the Bay materials is significant. The maximum heads/water levels increase as well as the degree of saltwater intrusion. With no SLR, the maximum head again occurs at the eastern boundary. However, for a 1 m SLR, the maximum head shifts westward to approximately $x = 650$ m; the head is 3.6 m. The 2 m SLR scenario, further shifts the maximum head to $x = 1650$ m; the maximum head is 3.8 m. The location of the maximum head is double that of the homogeneous case.

Similar saltwater intusions trends occur in the location of the 50% isochlor. For example, in the base case (no SLR), the 50% isochlor is located at $x = 4752$ m. A 1 m increase in the sea level boundary conditions, shifts the 50% isochlor location 50 m eastward, $x = 4702$ m. A 2 m increase in the coastal boundary, further increases saltwater intrusion. The 50% occurs at $x = 4242$ m.

5.3 Scenario 3 Results

In the third Scenario, the Bay deposits extend over 75% of the entire thickness of the aquifer (Figure 6). As in the previous Scenario, the inhomogeneity impacts both SLR in terms of the maximum head/water level, and seawater intrusion. The location of the 50% isochlor for 0 m, SLR conditions is $x = 4669$ m. This is over 200 m more landward than the homogeneous case. For a 1 m increase in SLR, the 50% isochlor shifts another 58 m landward, $x = 4612$ m. The location of the 50% isochlor occurs at $x = 4551$ m for the maximum SLR (2 m). The results indicate that the more extensive the Bay materials are, the greater is the degree of saltwater intrusion.

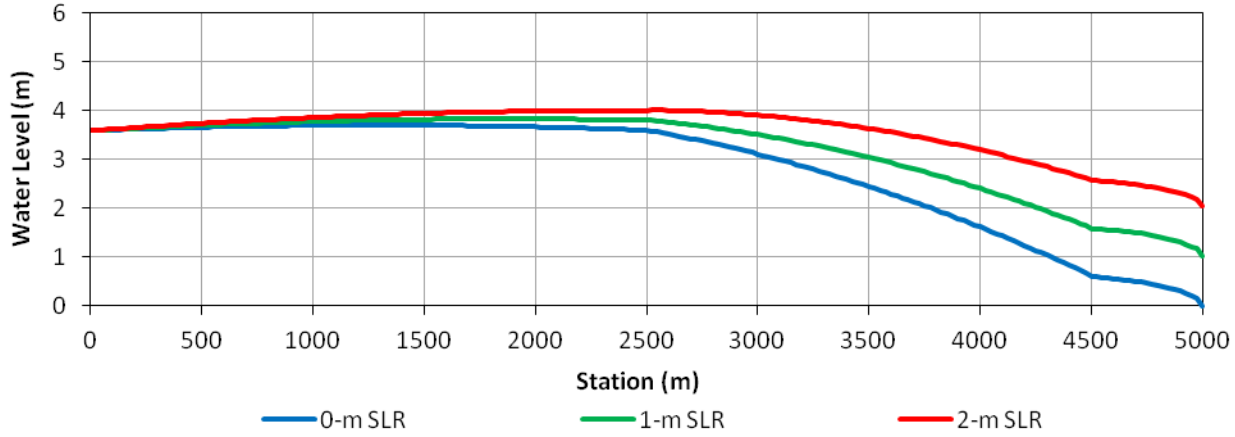

Figure 6 Scenario 4 water levels for 0, 1, and 2 m of sea level rise.

The maximum head in Scenario 3 also increases throughout the cross-sectional model. For example, with no SLR, the maximum head occurs at $x = 1275$ m; the head is approximately 3.7 m. With a 1 m SLR, the maximum head increases to 3.8 m and shifts westward to $x = 1850$ m. The maximum impact occurs at an assumed 2 m SLR. The maximum head is now over 4 m; the location is $x = 2525$ m.

In comparison with Scenario 1, the inhomogeneity dramatically increases both the maximum head and its location. The maximum head, in comparison with Scenario 1, is 1700 m further west. The maximum head has increased by over 0.2 m.

5.4 Scenario 4 Results

Scenario 4 examines the fully time dependent saltwater intrusion, SLR problem. The aquifer is assumed to be homogeneous. In contrast to the previous Scenarios, the initial conditions represent the actual, steady-state pressures and concentrations. These initial conditions were obtained from the steady-state pressure and concentrations of Scenario 1. SUTRA reads these data, the initial conditions, via a “restart" file.

The coastal boundary condition in this Scenario increases linearly over a 100 year period. The maximum SLR (2 m) occurs at the end of 100 years. An additional 25 years (a total of 125 years) were also simulated. In contrast to the previous Scenarios, the computational time significantly increased. Simulation times averaged 25 minutes for the first scenario; in Scenario 4 the total simulation required in excess of 12 hours of computer time (i7 processor). The time dependent boundary condition was implemented in SUTRA using subroutine “BCTIME."

The results of the time-dependent solution are indistinguishable from Scenario 1. The maximum heads occurring at the end of 50, and 100 years are virtually identical to the steady-state Scenario 1 simulations. The locations of the maximum heads are also the same. The saltwater intrusion pattern exhibits a similar pattern as Scenario 1.

These results confirm that the conceptual aquifer system reaches steady-state or equilibrium conditions within 25 years.

5.5 Scenario 5 Results

Scenario 5 examines the possible impact of a reduction in the annual recharge by 50% assuming SLR is 2 m. The Bay materials are 75% of the aquifer’s thickness (see Figure 3). Results are presented in Table 3 and Table 4. Reduced natural recharge increases saltwater intrusion. The location of the 50% isochlor is 4396 m from the eastern boundary; this represents the maximum intrusion occurring in all the simulation results. The maximum head (Table 4) is located at 1800 m. The decrease in the maximum head, despite the SLR, is a direct consequence of the reduction in natural recharge.

6 Conclusions

This investigation has developed a conceptual, density-dependent simulation model for the Eureka-Arcata plain. The model incorporates boundary conditions that reflect the limited existing data available for the area. The results of the conceptual modeling study have demonstrated:

a. Sea level rise can be expected to impact the study area.

b. The greater the magnitude of sea level rise, the more pronounced is the hydrologic impact.

c. Sea level rise increases the degree of saltwater intrusion (the location of the 50% isochlor) in all simulated scenarios.

d. Sea level rise shifts the location of the maximum hydraulic head westward.

e. The inhomogeneity in the intrinsic permeability significantly increases the impact of saltwater intrusion and the aquifer's water levels.

f. The greatest impact of SLR occurs when the Bay materials are assumed to be 75% of the aquifer's thickness.

g. The inclusion of groundwater extractions in the simulation model can be expected to increase saltwater intrusion especially with medium inhomogeneity.

h. A 50% decrease in natural recharge increases the saltwater intrusion in the aquifer. This assumes a SLR of 2 m; the thickness of the Bay materials is 22.5 m (75% of the total thickness).

7 Recommendations

The development of the conceptual model is based on a number of assumptions, for example, constant thickness, homogeneous, two-dimensional (in the vertical). It is recommended that additional data and/or studies be conducted to relax the modeling assumptions, and refine the modeling results. For example, the most significant parameter in the study is the intrinsic permeability of the Bay materials. Additional work is necessary to define both the lateral and vertical extent of these materials. Secondly, the recharge estimates used are based on long-term averages. Previous studies indicate that there may be a correlation between sea level rise and recharge. Such scenarios should be incorporated in future work. Thirdly, the cross-sectional model represents a single, uniform cross-section. A more realistic simulation model is inherently three dimensional. SUTRA has this capability, but the data requirements, even for a conceptual model, are far greater than both time and budget constraints of this investigation. Fourthly, in a three-dimensional model, it is possible to directly couple the surface water hydraulics of the Bay with the groundwater environment. Fifthly, pumping data should be developed and incorporated in the mathematical model. It can be expected that these additional stresses will increase saltwater intrusion, and potentially the impacts of SLR. All of these considerations would provide a more realistic assessment of the impact of sea level rise in the Eureka–Arcata plain.

8 References

1) Voss, C.I. and Alden M. Provost, "Sutra: A Model for Saturated-Unsaturated Variable-Density Groundwater Flow with Solute or Energy Transport," U.S. Geological Survey, *Water Resources* Investigation Report 02-4231, Reston, Virginia, 2010.

2) Harbaugh, A.W., “MODFLOW-2005, The U.S. Geological Survey Modular Groundwater Model–The Groundwater Flow Process," U.S. Geological Survey, *Techniques and Methods 6-A16*, Reston, Virginia, 2005.

3) Langevin, C.D., Thorne, D.T., Jr., Dausman, A.M., Sukip, M.C., and Weixing Guo, “SEAWAT Version 4: A Computer Program for Simulation of Multi-Species Solute and Heat Transport," U.S. Geological Survey, *Techniques and Methods, Book 6, Chapter A22*, Reston, Virginia, 2007.

4) Tony, N. Kiran and Sindhu, G., “Effect of Sea Level Rise on Ground Water Flow Modelling," 10th National Conference on Technological Trends (NCTT09), November 2009.

5) Chang, Sun Woo, “Dynamics of Saltwater Intrusion Processes in Saturated Porous Media System," a dissertation submitted in partial fulfillment for the Degree of Philosophy, Auburn University, Auburn, Alabama, 2012.

6) Oki, S.S. Souza, W.R., Bolke, E.L. and G.R. Bauer, “Numerical Analysis of Groundwater Flow and Salinity in the Ewa Area, Oahu, Hawaii," U.S. Geological Survey Open File Report 96-442, Honolulu, Hawaii, 1996.

7) Ghassemi, F., Molson, J.W., Falkland, A. and K. Alam, “Three-Dimensional Simulation of the Home Island Freshwater Lens: Preliminary Results," *Environmental Modelling and Software*, 14:181-190, 1999.

8) Ghassemi, F. and A.J. Jakeman, “Mathematical Modelling of Sea Water Intrusion, Nauru Island," *Hydrological Processes*, 4:269-281, 1990.

9) Loaiciga, H.A., Pingel, T.J., and E.S. Garcia, “Sea Water Intrusion by Sea-Level Rise: Scenarios for the 21st Century," *Ground Water*, 50(1):37-47, 2012.

10) Masterson, J.P. and S.P. Garabedian, *Ground Water*, 45(2):209-217, 2007.

11) Webb, M.D. and K. W.F. Howard, “Modeling the Transient Response of Saline Intrusion to Rising Sea-Levels," *Ground Water*, 49(4):560-569, 2011.

12) Rasmussen, P., Sonnenborg, T.O., Goncear, G. and K. Hinsby, “Assessing Impacts of Climate Change, Sea Level Rise, and Drainage Canals on Saltwater Intrusion to Coastal Aquifer," *Hdrol Earth Syst. Sci*., 17:421-443, 2013.

13) Werner, A.D. and C, Simmons, “Impact of Sea-Level Rise on Sea Water Intrusion in Coastal Aquifers," *Ground Water*, 47(2):197-204, 2009.

14) Langevin, C.D. and A.M. Dausman, “Numerical Simulation of Saltwater Intrusion in Response to Sea-Level Rise," U.S. Geologic Survey, Florida Integrated Science Center—Water and Restoration Studies, Miami, Florida, 2005.

15) Nishikawa, T., Siade, A.J., Reichard, E.G., Ponti, D.J., Canales, A.G., and T.A. Johnson, "Stratigraphic Controls on Seawater Intrusion and Implications for Groundwater Management, Dominguez Gap area of Los Angeles, California, USA," *Hydrogeology Journal*, 17:1699-1725, 2009.

16) Bjerklie, D.M., Mullaney, J.R., Stone, J. R., Skinner, B.J., and M.A. Ramlow,"Preliminary Investigation of the Effects of Sea-Level Rise on Groundwater Levels in New Haven, Connecticut," U.S. Geological Survey, *Open File Report 2012-1025*, Reston, Virginia, 2012.

17) Yechiele, Y., Shalev, E., Wollman, S. Kiro, Y, and U. Kafri, "Response of the Mediterranean and Dead Sea Coastal Aquifers to Sea Level Variations," *Water Resources Research*, 46, W12550, 2010.

18) Rozell, D.J. "Quantifying the Impact of Global Warming on Saltwater Intrusion at Shelter Island, New York Using a Groundwater Flow Model," A final report presented to the graduate school in partial fulfillment for the requirements for the Degree Master's of Science in Hydrogeology, Sony Brook University, 2007.

19) Bobba A.G., "Numerical Modelling of Salt-Water Intrusion due to Human Activities and Sea-Level Change in the Godavari Delta, India," *Hydrologic Sciences*, 47(S), S67-S80m 2002.

20) Evensen, R. E., "Geology and Groundwater Features of the Eureka Area, Humboldt County, California," U.S. Geological Survey, *Water Supply Paper 1470*, Washington, 1959.

21) California Department of Water Resources, *Bulletin 118*, 2003.

22) Johnson, M.J., "Ground-Water Conditions in the Eureka Area, Humboldt County, California, 1975, U.S. Geologic Survey, *Water-Resources Investigation Report: 78-127*, 1978.

23) California Department of Water Resources, "North Coastal Hydrographic Area," *Bulletin No. 142-1*, Sacramento, California, 1965.

24) California Department of Water Resources, California Water Plan, Volume 3, 2005.

25) California Department of Water Resources, California Water Plan, *Bulletin 160-09*, Volume 3, 2009.

26) Kelley, F.R., 1984, DMG Open-File Report 84-38, Geology and Geomorphic Features Related to Landsliding, Arcata North 7.5' Quadrangle, Humboldt County, California Scale 1:24,000.

27) Kilbourne, R.T., 1985, DMG Open-File Report 85-04, Geology and Geomorphic Features Related to Landsliding, Fields Landing 7.5' Quadrangle, Humboldt County, California Scale 1:24,000.

28) Kelley, F.R., 1984, DMG Open-File Report 84-39, Geology and Geomorphic Features Related to Landsliding, Arcata South 7.5' Quadrangle, Humboldt County, California Scale 1:24,000.

29) R.J. McLaughlin, S.D. Ellen, M.C. Blake, Jr., A.S. Jayko, W.P. Irwin, K.R. Aalto, G.A. Carver, and S.H. Clarke, Jr. Digital Database by J.B. Barnes, J.D. Cecil, and K.A. Cyr, Geology of the Cape Mendocino, Eureka, Garberville, and Southwestern Part of the Hayfork 30 X 60 Minute Quadrangles and Adjacent Offshore Area, Northern California, Figure 5, Sheets 1, 4, U.S. Geologic Survey, 2000.

30) R.G. Strand, "Geologic Map of California Redding Sheet," California Dividing of Mines and Geology, Scale 1:250,000, 1962.

31) California Department of Water Resources, Well Data, Eureka-Arcata Plain, 2013.

32) National Oceanic and Atmospheric Administration, National Climatic Data Center (NCDC). (ncdc.noaa.gov), 2013.

33) California Department of Water Resources, California Irrigation Management Information System (CIMIS), (water.ca.gov/cimis), 2013

34) California Department of Water Resources, California Data Exchange Center (CDEC), (http://cdec.water.ca.gov), 2013.

35) Northern Hydrology & Engineering, Jeff Anderson, personal communications, 2013, 2014.

36) Willis, R. and William W-G. Yeh, *Groundwater Systems Planning and Management*, Prentice-Hall, Inc., Englewood-Cliffs, New Jersey, 1987.